Dual-Array Based MPPT for Grid-Connected Photovoltaic Systems

Darko Ostojić, Gabriele Grandi, and Darko Marčetić

Abstract—**A novel maximum power point tracking (MPPT) algorithm for three-phase grid-connected photovoltaic (PV) generation systems is presented in this paper. Reference is made to a conversion scheme consisting in two balanced arrays of PV modules, each one feeding a standard 2-level three-phase voltage source inverter (VSI). The dc-link voltages of each VSI are regulated according with the requirement of the proposed MPPT algorithm, based on the comparison of the operating points of the two PV arrays. Inverters are connected to grid by a three-phase transformer with open-end windings configuration on inverters side. The resulting conversion structure performs as a power active filter, doubling the power capability of a single VSI, with the additional benefit of multilevel voltage waveforms. The proposed MPPT algorithm has been successfully verified by experimental tests.**

Index Terms—**Photovoltaic power systems, multilevel inverters, maximum power point trackers.**

I. Introduction

PHOTOVOLTAIC (PV) energy sources have been initially developed for small-power and portable applications. However over the last two decades there was strong trend towards high-power plants with peak power reached 60 MW [1]]. This new field demands specific topologies and power electronic converters research, together with new control methods. Multilevel converters already applied for high-power drives are finding their way in this PV application, bringing benefits such are lower *dv/dt* and reduced harmonic distortion of the output voltage.

Another indispensable issue for PV plants is provision of maximum output power. Due to strong nonlinear characteristic of PV cell, a maximum power point tracking (MPPT) control algorithm is utilized to maximize conversion of available solar energy. A considerable number of techniques have been developed with a particular expansion in the last decade and the interest of the research community remains strong [2]. Still, different MPPT techniques suit different applications depending also on the topology and the rated power. In this paper, the dual VSI topology [3] is considered, and a novel MPPT algorithm has been applied to maximize power injection into

the grid, according to the block diagram of Fig. 1. The two standard two-level VSI are connected to open-end primary windings of a standard three-phase transformer. The whole PV field is shared into two equal arrays, with each inverter directly wired with one of the PV arrays. The secondary windings are connected to the grid with a traditional star (or delta) configuration. Note that the transformer contributes with its leakage inductance to the ac-link inductance which is always necessary for the grid coupling of a VSI. Furthermore, the presence of a low-frequency transformer enable the direct connection of high power generation systems to either medium- or high-voltage grids (10 kV or more). The resulting three-phase converter is able to operate as a voltage multilevel inverter, equivalent to a three-level inverter, with corresponding multilevel benefits.

Strictly speaking, only permanent sweeping of the V-I characteristic can determine exact position of the MPP in every instant for all the circumstances (different irradiance, shading and temperature). However, this mode of constant perturbation is unacceptable for application, leading to development of many "approximate" methods today commonly accepted under name MPPT. It can be noted that "sweep" can represent the appropriate method in some cases (e.g. for low-power applications if performed in regular and not so often intervals) [3]. Generally, methods can be divided in two classes, based on type of the applied loop.
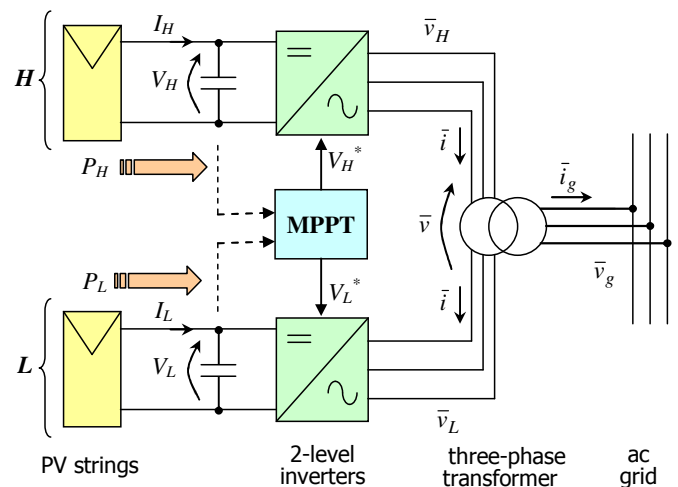

Fig. 1. Block diagram of the dual VSI topology including an open-winding three-phase transformer.

D. Ostojić and G. Grandi are with Alma Mater Studiorum – University of Bolonja, Department of Electrical Engineering, Bologna, Italy (e-mail: darko.ostojic@mail.ing.unibo.it).

D. Marčetić is with the University of Novi Sad, Faculty of Technical Sciences, Novi Sad, Serbia (e-mail: dramar@uns.ac.rs).

1) Open loop control, using *a priori* model of the panel behavior (usually eventually updated). Basic representatives are
   - application of pilot cells [2],
   - open-circuit voltage/short-circuit current based methods [4],
   - model (parameter) based methods [5], particularly "one cycle control" [6].
2) Closed loop control, since they compare the current state with previous in order to determine position of the MPP. Basic representatives are
   - perturb and observe (P&O, sometimes called "hill climbing") [7],
   - incremental conductance (INC) [8],
   - fuzzy logic and Neural network [9], [10],
   - ripple correlation control (RCC) [11],
   - load current/voltage maximization [12],
   - sliding mode control [13].

Among all the methods most of the focus has been on P&O and INC method. They practically established themselves as almost standard methods due to their simplicity and ease of application. Other methods such are fuzzy logic and neural networks are more complex to implement and require field-specific tuning. P&O usually uses PV power, but it has been shown that output electric parameters of the converter can be used as well [12]. The MPPT algorithm proposed in this paper is based on a forced small displacement in the working points of two identical PV arrays, allowing sharing of data between them on the basis of instantaneous currents measurement. Similar MPPT schemes have been recently presented in [14] and [15], but with reference to different PV conversion structures.

II. CONVERTER AND CONTROL SYSTEM

In the present case of PV applications, the proper inverter dc voltage range can be obtained by adjusting the number of series-connected modules for each PV array (string), avoiding the use of intermediate dc/dc choppers. In this case, inverters regulate dc-bus voltages according to the MPPT requirements, as explained in the following. With reference to the scheme of Fig. 1, using space vector representation, the output voltage vector of the multi-level converter is given by the contribution of the voltage vectors   and , generated by inverter H and L respectively,

$$\bar{v} = \bar{v}_H + \bar{v}_L \tag{1}$$

$$\bar{v}_H = (2/3)V_H (S_{1H} + S_{2H} e^{j2\pi/3} + S_{3H} e^{j\pi 4/3}) \tag{2}$$

$$\bar{v}_L = -(2/3)V_L (S_{1L} + S_{2L} e^{j2\pi/3} + S_{3L} e^{j4\pi/3}) \tag{3}$$

where $\{S_{1H}, S_{2H}, S_{3H}, S_{1L}, S_{2L}, S_{3L}\} = \{0, 1\}$ are the switch states of the inverter legs [16]. Fig. 2 shows the corresponding voltage space vectors.

The conversion system is symmetric, having both inverters with equal ratings and two equal groups (arrays) of PV modules supplying them. The dc bus voltage references
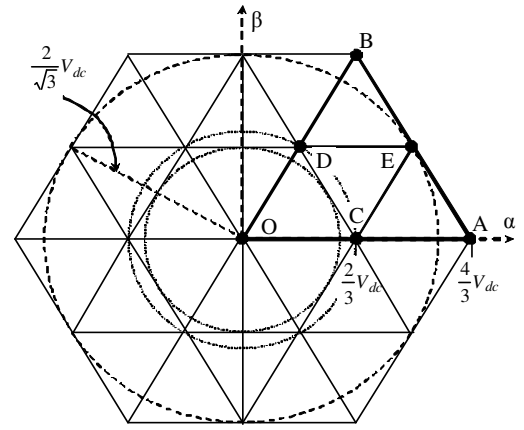

Fig. 2. Dual inverter voltage vector plot in case $V_H = V_L = V_{dc}$.

generated by the MPPT controller, V_H^* and V_L^*, are very close one to the other, as discussed in the next section. Two distinct voltage controllers have been implemented, according with the block diagram shown in Fig. 3. In particular, the two dc voltages (V_H, V_L) are regulated by two controllers, here called "sigma" (Σ) and "delta" (Δ). The voltage controller Σ acts in order to regulate the average value of dc bus voltages, V_{dc} (i.e., their sum), whereas the voltage controller Δ acts in order to set the difference between the dc bus voltages (ΔV). The input signals of both voltage controllers, V_Σ and V_Δ, can be built by adding and subtracting one from the other the individual dc voltage errors ΔV_H and ΔV_L, as follows

$$V_\Sigma = \Delta V_H + \Delta V_L = (V_H + V_L) - (V_H^* + V_L^*) \tag{4}$$

$$V_\Delta = \Delta V_H - \Delta V_L = (V_H - V_L) - (V_H^* - V_L^*) \tag{5}$$

being:

$$\begin{cases} \Delta V_L = V_L - V_L^* \\ \Delta V_H = V_H - V_H^*. \end{cases} \tag{6}$$

The voltage controller Σ directly generates the current reference for the dual inverter, I^*, corresponding to the active power injected into the grid, regardless to the power sharing between the two inverters "H" and "L", as shown in Fig. 3. If the ac current is in phase with the grid voltage, the resulting current space vector reference is

$$\bar{i}^* = I^* \hat{v}_g \tag{7}$$

being $\hat{v}_g$ the unity space vector of the grid voltage. It can be noted that reactive and/or harmonic compensation current references can be included in (7) if active power filter operation is required.

To solve the problem of current control in grid-connected application a simple proportional controller with a feed-forward action (grid voltage) has been adopted, due to its simplicity, good dynamic response and immunity to harmonic disturbance. In particular, the reference voltage is calculated as

$$\bar{v}^* = K_c (\bar{i}^* - \bar{i}) + \vec{v}_g' \tag{8}$$

being $\vec{v}_g'$ the space vector of the grid voltage at the inverter side.
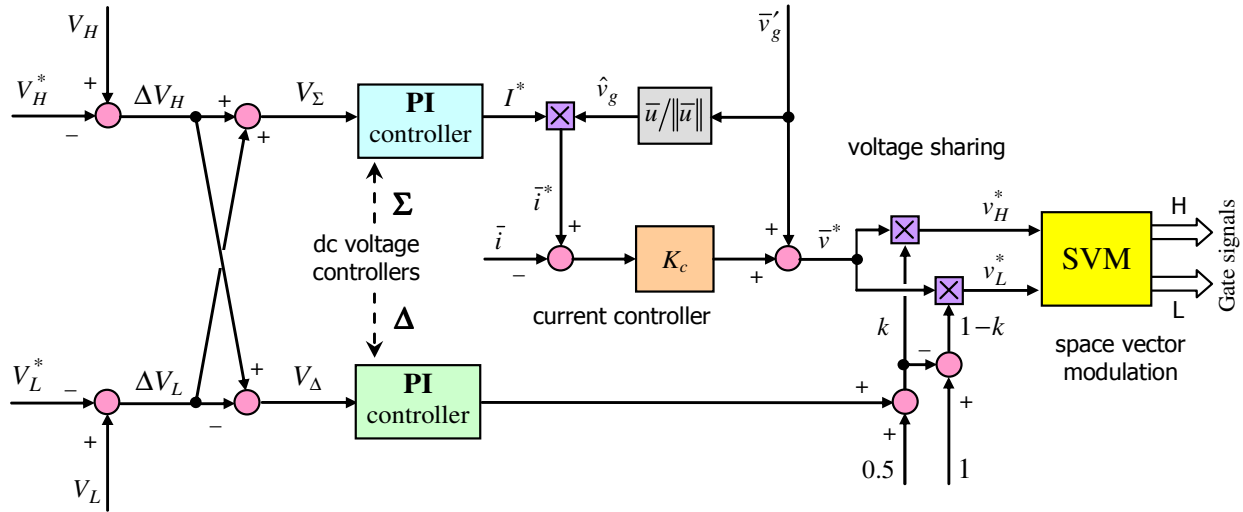
Fig. 3. Schematic diagram of proposed control system.

Being the converter supplied by two distinct PV arrays, it is necessary to regulate the power flow from the two sources. A possible approach to achieve the power sharing control is to define the decomposition of the total reference into two collinear vectors [3]:

$$\begin{cases} \overline{v}_H^* = k\,\overline{v}^* \\ \overline{v}_L^* = (1-k)\,\overline{v}^*. \end{cases} \tag{9}$$

The condition (9) allows maximum dc voltage utilization. Being the output ac current of the two inverters the same, the coefficient k also defines the power sharing between the two inverters. In terms of averaged values within the switching period, the output power can be expressed as

$$p = \frac{3}{2}\overline{v}^*\overline{i} = p_H + p_L \tag{10}$$

where p_H and p_L are the individual powers from the two inverters. By combining (9) with (10) leads to

$$\begin{cases} p_H = \dfrac{3}{2}\overline{v}_H^* \cdot \overline{i} = k\,p \\ p_L = \dfrac{3}{2}\overline{v}_L^* \cdot \overline{i} = (1-k)\,p. \end{cases} \tag{11}$$

Once the inverter reference voltages $\overline{v}_H^*$ and $\overline{v}_L^*$ are determined by (9), they must be synthesized by the dual two-level inverter and applied to the open-end windings of the transformer. A SVM providing proper voltage multilevel waveforms and avoiding double simultaneous commutations have been presented in [16]. This method leads to switching sequences that can be implemented in the sole PWM generation unit of an industrial DSP which usually provides a unique carrier for all three phases. It has been achieved by introducing asymmetrical PWM pattern to avoid different carriers. This new algorithm has been adopted here.

III. PROPOSED MPPT ALGORITHM

The well-known problem of the maximum power point tracking consists in finding the MPP voltage, V_{MPP} (or the MPP current, I_{MPP}), at which the PV field provides the maximum output power, P_{MPP}. MPP continuously moves, according to variations in environmental conditions (i.e. solar irradiation and cell temperature). Among the numerous known solutions [2], [4]–[15], the one proposed in [14], [15] is particularly suitable for the dual inverter configuration, due to the presence of two identical groups of PV modules. The algorithm is based on deliberate introduction of a small difference ΔV^* (in the order of %) between reference voltages of the two PV fields V_H^* and V_L^*, as follows

$$V_L^* = K_v\,V_H^* \tag{12}$$

$$\Delta V^* = V_H^* - V_L^* = (1-K_v)\,V_H^* \tag{13}$$

where the coefficient K_v slightly differs from 1 ($K_v \cong 0.95\text{-}0.98$). Due to the particular shape of power vs. voltage characteristic (P-V curve), the powers generated by the two PV fields, P_L and P_H, practically coincide if the operating points are on the "flat" in neighborhood of MPP, according to Fig. 4a. Conversely, on "sloped" parts of the P-V curve, one of the powers is higher than the other, or vice-versa, depending on the position of the operating points with respect to the MPP. In particular, the following three possibilities occur:

$$\begin{cases} P_L < P_H & \Rightarrow & V < V_{MPP} \\ P_L = P_H & \Rightarrow & V \cong V_{MPP} \\ P_L > P_H & \Rightarrow & V > V_{MPP}. \end{cases} \tag{14}$$

In effect, the difference between P_H and P_L gives an estimation of the slope of the P-V characteristic:

$$\frac{dP}{dV} \cong \frac{P_H - P_L}{(1-K_v)V_H} \cong K_p\left(P_H - P_L\right). \tag{15}$$

Hence, reference dc voltages V_H^* and V_L^* can be found as the output of a simple PI-controller acting on the error between the two powers, as represented in Fig. 4b.

The choice of a proper value for K_v is a tradeoff between efficiency, which is higher as K_v approaches 1, and immunity to both noise and PV modules asymmetry, which increase as
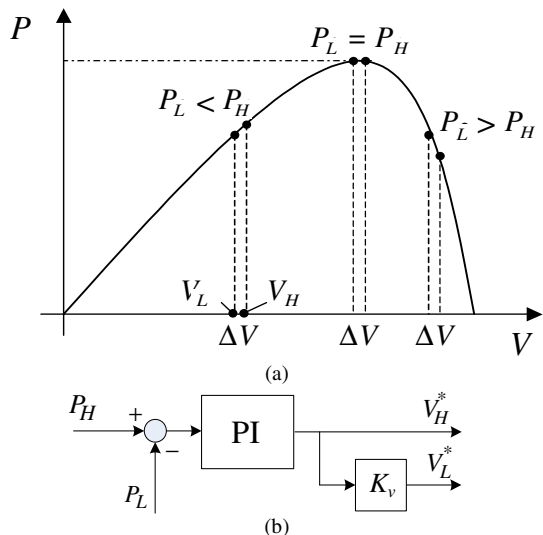
(a)

(b)

Fig. 4. Principle of MPPT algorithm: (a) P-V diagram, (b) control scheme.

Fig. 5. Arrangement of 6+6 PV modules on the roof.

K_v diverge from 1. Obviously, the proposed algorithm is based on the assumption that the two PV arrays have the same P-V (or I-V) characteristic. For this reason, the PV arrays should consist of equal number and same type of PV modules. In spite of P-V characteristics of two identical PV modules slightly differ one from the other (the dispersion is in the order of few %), when many PV modules are arranged in two big arrays, their global P-V characteristics are averaged and practically coincides. On the basis of (2) and (3), the effects of PI regulators Σ and Δ lead to the following steady-state conditions

$$V_\Sigma = 0 \quad \Rightarrow \quad V_H + V_L = V_H^* + V_L^* \tag{16}$$

$$V_\Delta = 0 \quad \Rightarrow \quad V_H - V_L = \Delta V^*. \tag{17}$$

IV. EXPERIMENTAL RESULTS

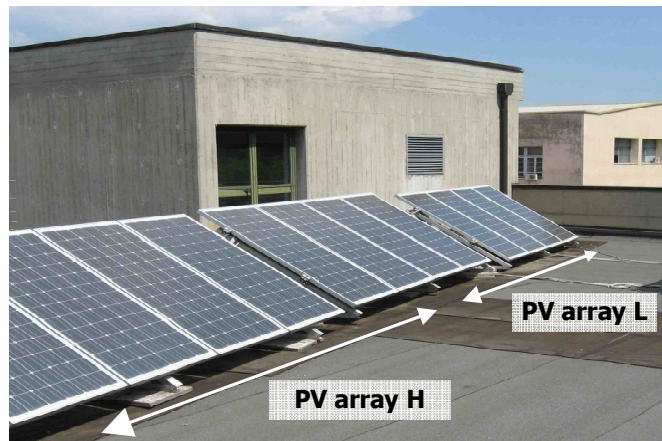To ensure the safety, the system has been implemented by using only parallel connections of PV modules, since the presence of a grid-transformer with the proper turn ratio enables voltage adaptation. The resulting PV array voltage range is the same of a single PV module, in the range 20−40 V, allowing use of low-voltage MOSFETs. These types of switches are cheap, being widely used in automotive applications, and they feature good efficiency, since its on-state resistance is a strong decreasing function of the blocking voltage rating. The main characteristics of the whole PV generation system prototype are summarized in Table I, and some pictures of the experimental set-up are given in Fig. 5. Reference is made to the scheme presented in Fig. 1, with the two PV arrays consisting each in six PV modules in parallel, directly connected to the inverters. The experimental results show the action of the MPPT controller with reference to opposite voltage starting conditions with respect to the MPP voltage (V_{MPP}). In all experiments a coefficient $K_v = 0.98$ has been selected, leading to a small difference between V_H and V_L, about 0.5 V.

Fig. 6 shows the transient to the MPP starting from the open-circuit voltage (Fig. 6a in time domain, Fig. 6b in I-V diagram).

Fig. 7 shows the transient to the MPP starting from the minimum dc voltage. Steady states and settling times are proving that also with a very small voltage displacement a
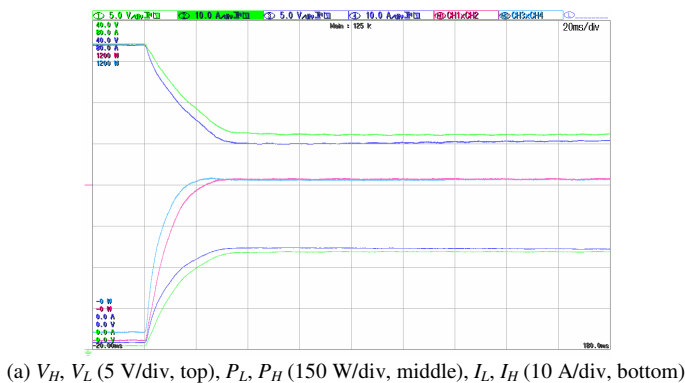
(a) V_H, V_L (5 V/div, top), P_L, P_H (150 W/div, middle), I_L, I_H (10 A/div, bottom)
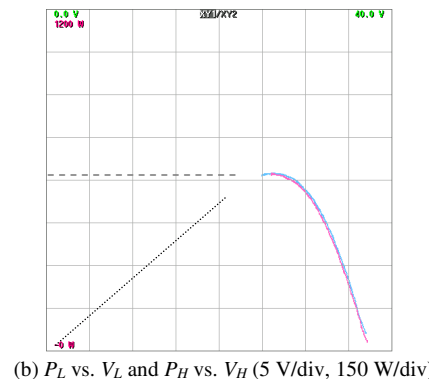
(b) P_L vs. V_L and P_H vs. V_H (5 V/div, 150 W/div)

Fig. 6. Experimental results: transient from no-load to MPP with Kv =0.98.

(a) V_H, V_L (5 V/div, top), P_L, P_H (150 W/div, middle), I_L, I_H (10 A/div, bottom)

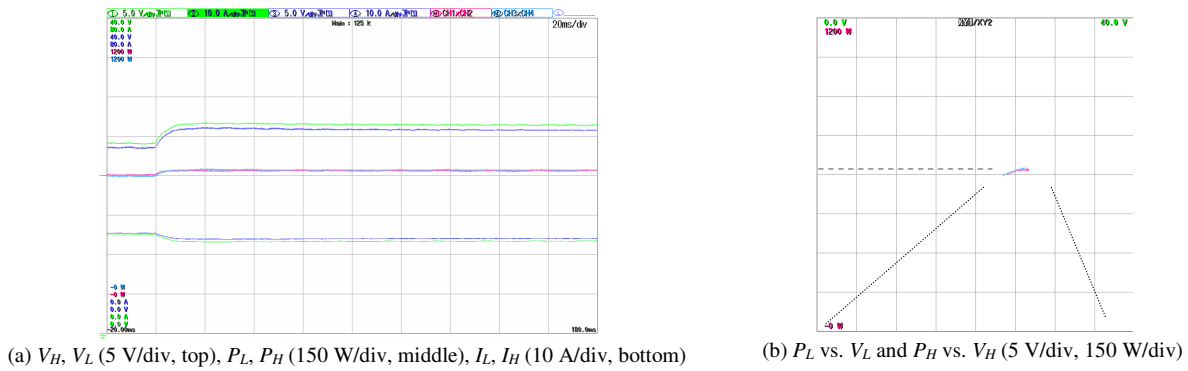(b) P_L vs. V_L and P_H vs. V_H (5 V/div, 150 W/div)

Fig. 7. Experimental results: transient from minimum dc voltage to MPP with K_v =0.98.

satisfactory behavior of the MPPT algorithm can be obtained, reached without oscillations in about 40 ms. In all the examined cases, both the steady-state powers PH and PL practically coincide with the MPP, proving the effectiveness of

TABLE I
MAIN PARAMETERS OF THE CONVERTER

INVERTERS	
configuration (H and L)	two-level VSI
MOSFETs (6 in parallel per switch)	IRF2807
MOSFETs ratings	V_{DSS}=75[V]; R_{DS}=13[mΩ]
dc-bus capacitance	23 [mF]
switching frequency	20 [kHz]
TRANSFORMER and GRID	
turn ratio	230/24 [V/V]
converter/grid-side winding connection	open ends/star
rated power	1500 [VA]
short circuit voltage	6.9 [%]
ac link inductance (converter side)	0.4 [mH]
grid voltage (line-to-line), frequency	250 [V], 50 [Hz]

the proposed MPPT algorithm.

V. CONCLUSION

The MPPT algorithm proposed in this paper is based on the comparison of the operating points of two PV arrays, each one directly connected to a standard 2-level three-phase inverter. This method shows good results applying considerably low difference between the two PV array voltages. The coefficient K_v represents a degree of freedom that can be tuned depending on different conditions or demanded dynamic response. It is suitable for application for high-power applications where V-I characteristics of two groups are expected to be quite similar by the law of large numbers. The measuring system might require initial tuning (calibration). The case of different characteristics due to partial shadowing is not of importance for high-power application since the installation is projected to avoid such a problem.

REFERENCES

[1] Denis Lenardič, "Large-Scale Photovoltaic Power Plants – Annual Review 2008," pp. 11−15, May 2009. [Online]. Available: www.pvresources.com.

[2] T. Esram, P. Chapman, "Comparison of photovoltaic array maximum power point tracking techniques," IEEE Trans. Energy Convers., Vol. 22, No. 2, pp. 439–449, June 2007.

[3] G. Grandi, D. Ostojic and D. Casadei, "A novel DC-voltage regulation scheme for dual-inverter grid-connected photovoltaic plants," in Conf. Rec. IEEE Electromotion 2009, pp. 1−6.

[4] M. Masoum, H. Dehbonei, and E. Fuchs, "Theoretical and experimental analyses of photovoltaic systems with voltage and current-based maximum power-point tracking," IEEE Trans. Energy Convers., Vol. 17, No. 4, pp. 514–522, Dec. 2002.

[5] W. Xiao, W. Dunford, P. Palmer, and A. Capel, "Regulation of photovoltaic voltage," IEEE Trans. Ind. Electron., Vol. 54, No. 3, pp. 1365–1374, June 2007.

[6] M. Fortunato, A. Giustiniani, G. Petrone, G. Spagnuolo, and M. Vitelli, "Maximum power point tracking in a one-cycle-controlled single-stage photovoltaic inverter," IEEE Trans. Ind. Electron., Vol. 55, No. 7, pp. 2684–2693, Jul. 2008.

[7] N. Femia, G. Petrone, G. Spagnuolo, and M. Vitelli, "Optimization of perturb and observe maximum power point tracking method," IEEE Trans. Power Electron., Vol. 20, No. 4, pp. 963–973, Jul. 2005.

[8] F. Liu , S. Duan , F. Liu , B. Liu and Y. Kang "A variable step size INC MPPT method for PV systems," IEEE Trans. Ind. Electron., Vol. 55, No. 7, pp. 2622−2628, Jul. 2008.

[9] T. Kottas, Y. Boutalis, and A. Karlis, "New maximum power point tracker for PV arrays using fuzzy controller in close cooperation with fuzzy cognitive networks," IEEE Trans. Energy Conv., Vol. 21, No. 3, pp. 793–803, 2006.

[10] A. Varnham, A. Al-Ibrahim, G. Virk, D. Azzi, "Soft-Computing Model-Based Controllers for Increased Photovoltaic Plant Efficiencies," IEEE Trans. on Energy Conv., pp. 873−880, Vol. 22, No. 4, Dec. 2007.

[11] D. Casadei, G. Grandi and C. Rossi, "Single-phase single-stage photovoltaic generation system based on a ripple correlation control maximum power point tracking," IEEE Trans. Energy Convers., Vol. 21, No. 2, pp. 562−568, June 2006.

[12] D. Shmilovitz, "On the control of photovoltaic maximum power point tracker via output parameters," in IEE Proc. Electr. Power Appl., Vol. 152, No. 2, Mar. 2005.

[13] C. C. Chu and C. L. Chen, "Robust Maximum Power Point Tracking Method for Photovoltaic Cells: a Sliding Mode Control Approach," Solar energy, 2009 (in press).

[14] J.-H. Park, J.-Y. Ahn, B.-H. Cho and G.-J. Yu, "Dual-Module-Based Maximum Power Point Tracking Control of Photovoltaic Systems," IEEE Trans. Ind. App., Vol. 53, No. 4, pp. 1036−1047, June 2006.

[15] G. Grandi, C. Rossi, G. Fantini, "Modular Photovoltaic Generation Systems Based on a Dual-Module MPPT Algorithm," in Conf. Rec. IEEE ISIE 2007, pp. 2432−2436.

[16] G. Grandi, C. Rossi, D. Ostojic, and D. Casadei, "A New Multilevel Conversion Structure for Grid-Connected PV Applications," IEEE Trans. Ind. Electron., Vol. 56, No. 9, Nov. 2009.